Microstructure based effective stress formulation for partially saturated granular soils

K.N. Manahiloh[1], B. Muhunthan[2], and W.J. Likos[3]

Abstract

The principle of effective stress states that the strength and volume change behaviors of soil are governed by intergranular forces expressed in terms of a continuum quantity called effective stress. Although the principle of effective stress is regarded as one of the most fundamental concepts in soil mechanics, its applicability to partially saturated soil has been debated. The central issue is whether a measure can be developed for three-phase soils that plays an equivalent role as the effective stress does in two-phase soils. This study attempts to forward such a measure by incorporating soil microstructure in the effective stress formulation. A novel suction-controlled experimental setup is developed and integrated with an X-ray CT scanning system to image and model microstructural features. A tensorial quantity, called fabric tensor of the liquid phase, that characterizes the complex fabric resulting from saturated pockets and networks of liquid bridges is identified and introduced in the proposed formulation. It is shown that fabric tensor of the liquid phase varies randomly, in both the wetting and drying phases of the partial saturation, and has an intrinsic association with the evolution of the effective stress tensor. It is also shown that this random variation can be depicted by applying techniques of digital image processing. It is concluded that, for partially saturated granular soils, the consideration of fabric tensor of the liquid phase in effective stress formulations is imperative.

Keywords: Partial saturation, granular soil, effective stress, virtual work, soil fabric, fabric tensor, microstructure, soil suction, degree of saturation, X-ray computed tomography (X-ray CT), image processing, soil water retention curve (SWRC)

Citation Information: Please cite this work as follows
Manahiloh Kalehiwot, N., B. Muhunthan, and J. Likos William, *Microstructure-Based Effective Stress Formulation for Unsaturated Granular Soils.* International Journal of Geomechanics, 2016. **16**(6).

Official publication link: https://ascelibrary.org/doi/10.1061/%28ASCE%29GM.1943-5622.0000617

[1] A.M. ASCE, Ph.D., Assistant Professor, Department of Civil & Environmental Engineering, University of Delaware, 301 DuPont Hall, Newark, DE 19716, E-mail: knega@udel.edu
[2] F. ASCE, Ph.D., P.E., Professor, Department of Civil & Environmental Engineering, Washington State University, 405 Spokane St., Sloan Hall 30, Pullman, WA 99164, e-mail: muhuntha@wsu.edu
[3] M. ASCE, Ph.D., Associate Professor, Department of Civil & Environmental Engineering, University of Wisconsin-Madison, 2215 Engineering Hall, Madison, WI 53706, e-mail: likos@wisc.edu

Introduction

Terzaghi's principle of effective stress for saturated soils is regarded as one of the fundamental concepts in geotechnical practices and the marker for the birth of classical soil mechanics. This principle assumes two-phase media whose mechanical and hydraulic behaviors are unified by the effective stress (Terzaghi 1936).

$$\sigma_{ij}^{'} = \sigma_{ij} - u_w \delta_{ij} \tag{1}$$

Where: σ_{ij}, and $\sigma_{ij}^{'}$ are the total and effective stresses; and $u_w\delta_{ij}$ is the pore-water pressure.

For saturated soils, the validity of the effective stress principle has been experimentally verified (e.g. Rendulic 1936; Bishop & Eldin 1950; Laughton 1955; Skempton 1961; Wood 2005). However, as can be inferred from Equation 1, Terzaghi's effective stress principle does not capture the full behavior of as soil becomes partially saturated. In partially saturated soils, individual solid particles may be partially exposed to water and/or to air. Moreover in a state of partial saturation fluid exists at differing pressures depending on the degree of saturation at different locations throughout the soil microstructure. This variation in turn results in matric suction tensor $(u_a - u_w)\delta_{ij}$: a phenomenon that directly influences the net forces acting at particle-particle contacts.

Effective stress formulations for partially saturated soils

The study on the mechanical behavior of unsaturated soils, in relation to the effective stress, has shown significant developments since the 1950s (Croney et al. 1958; Bishop 1959) and 1960s (Lambe 1960; Aitchison 1961; Jennings 1961). Croney et al. (1958) suggested an effective stress formulation for unsaturated soils in which the pore-water pressure in the Terzaghi's expression for saturated soils is modified by a bonding factor β' as

$$\sigma_{ij}^{'} = \sigma_{ij} - \beta' \times u_w \delta_{ij} \tag{2}$$

Where $\sigma_{ij}^{'}$ and σ_{ij} are the effective and total normal stresses. β' is a measure of the number of bonds under tension effective in contributing to soil strength (Croney et al. 1958).

Bishop (1959) extended Terzaghi's unified effective stress principle to unsaturated soils by describing the stress state as a function of the pore-air pressure (u_a), pore-water pressure (u_w) and a parameter (χ) referred to as the "Bishop parameter" and related to the degree of saturation, *S*, of the soil as

$$\sigma_{ij}^{'} = \sigma_{ij} - u_a\delta_{ij} + \chi(u_a - u_w)\delta_{ij} \quad (3)$$

Jennings (1961) outlined two methods of measuring χ by comparing the behavior of a soil specimen under changes in externally applied pressure. Essentially similar experimental approaches for the measurement of the factor χ, and thus the relationship between χ and *S*, were suggested by other researchers (Bishop et al. 1960; Bishop & Donald 1961). The parameter χ attains values of 1 and 0 for fully saturated and fully dry soil conditions respectively. On the other hand, Coleman (1962) described χ as a parameter strongly related to the soil structure rather than to volumetric parameters like the degree of saturation. Following Coleman's assertion, recent studies (e.g. Khalili & Khabbaz 1998 ; Khalili et al. 2004) related χ to the ratio of soil matric potential to the air-entry value or the suction ratio. Lu and Likos (2004) referred to the product $\chi(u_a - u_w)\delta_{ij}$ as the suction stress and regarded the Bishop's effective stress approach as a macroscale interpretation attempting to describe the microscale contribution of interparticle pore-water menisci located between soil particles and physicochemical forces to the net interparticle stress. Furthermore, Lu and Likos (2004) extended Bishop's effective stress formulation and gave tensorial representation of suction stress for isotropic and anisotropic soils as Equations 4 and 5 respectively.

$$\chi(u_a - u_w)\delta_{ij} \quad (4)$$

$$\chi_{ij}(u_a - u_w)\delta_{ij} \quad (5)$$

The validity of Bishop's effective stress formulation for unsaturated soils over the whole range of saturation was contested by Jennings and Burland (1962). They claimed, even though the formulation is statically correct as indicated by Bishop and Donald (1961), it was not shown that the soil behavior is unaffected by changes in $(\sigma_a - u_a)\delta_{ij}$ and $\chi(u_a - u_w)\delta_{ij}$ such that their sum $(= \sigma'_{ij})$ is constant. They also showed that attempts to link the stress and deformation behavior of an unsaturated soil with a single-valued effective stress equation, as is the case of Bishop, have resulted in limited success. They found out that oedometer and all-around compression tests performed on unsaturated and saturated soils indicated no unique relationship between volume change and effective stress for most soils.

Alternative forms, that use independent stress state variables, were proposed to capture the mechanical and volumetric behavior of unsaturated soils (Coleman 1962; Aitchison 1973; Fredlund & Rahardjo 1993; Houlsby 1997; Li 2003a; Berney et al. 2004). In such formulations, constitutive relationships were implemented for soil structure and flow laws were applied for the fluids to characterize unsaturated behavior. Many of the proposed relationships (Aitchison 1961; Jennings 1961; Aitchison 1973; Richards 1985), incorporate a soil parameter in order to come up with single-valued effective stress equations (i.e. one stress state variable). However, experiments (Fredlund & Rahardjo 1993) have demonstrated that relationships derived from measured soil properties do not turn out to be single-valued.

The problem with single-valued effective stress equations is that the effective stress will have different magnitudes for different problems (volume change or shear strength), different stress paths, and different soil types (Coleman 1962; Jennings & Burland 1962; Burland 1964). Even though the use of more than one stress state variable is tacitly agreed up on by many researchers,

the minimum number of variables for the investigation of saturated and unsaturated behaviors had been a topic of debate for many years (Zhang & Lytton 2006). (Coleman (1962); Burland (1965); Matyas and Radhakrishna (1968); Barden et al. (1969); Brackley (1971); Fredlund and Morgenstern (1977)) argue that it is important to use two or more stress state variables. Fredlund and Morgenstern (1977), conducting null tests, suggested that the possible combinations of stress state variables given by Equation 6 could be used in cases where the air pressure (u_a), the pore-pressure (u_w), and the total stress (σ) are assumed as references respectively. Houlsby (1997) illustrated the choice of stress variables as being arbitrary as long as corresponding strain variables satisfy work conjugacy.

$$\left.\begin{array}{l}(\sigma_{ij}-u_a\delta_{ij}) \text{ and } (u_a-u_w)\delta_{ij}\\ (\sigma_{ij}-u_w\delta_{ij}) \text{ and } (u_a-u_w)\delta_{ij}\\ (\sigma_{ij}-u_a\delta_{ij}) \text{ and } (\sigma_{ij}-u_w\delta_{ij})\end{array}\right\} \quad (6)$$

Referring to the preceding discussion it can be said, no matter how the unsaturated behavior is pictured, clear assumptions, scope descriptions and objectives must be put before further analyses are carried out. In this respect, Houlsby (2004) stressed the importance of clear assertions with regard to the specific aspect of mechanical behavior under investigation and he highlighted the importance of separating the effective stress formulation in to two stages: definition and hypothesis.

In general effective stress formulations suggested by past studies fall under the umbrella of: the single variable effective stress of the Bishop's type; formulations that involve multiple independent stress state variables (e.g. Fredlund & Rahardjo 1993); formulations that involve critical state considerations (Alonso et al. 1987; Alonso et al. 1990; Toll 1990; Wheeler & Sivakumar 1993, 1995; Vaunat et al. 2000); or formulations that combine unified effective stress of the Bishop type with additional stress variables which are functions of parameters such as

suction, soil fabric and saturation (e.g. Li 2003a; Alonso et al. 2010). Nuth and Laloui (2008) chronologically classified the evolution of effective stress formulations for unsaturated soils as follows.

i. Bishop's single effective stress of the form:

$$\sigma_{ij}^{'} = (\sigma_{ij} - u_a\delta_{ij}) + \chi\left(u_a - u_w\right)\delta_{ij} \tag{7}$$

ii. Independent stress variables with possible combinations:

$$\left.\begin{array}{l}(\sigma_{ij} - u_a\delta_{ij}) \text{ and } (u_a - u_w)\delta_{ij} \\ (\sigma_{ij} - u_w\delta_{ij}) \text{ and } (u_a - u_w)\delta_{ij} \\ (\sigma_{ij} - u_a\delta_{ij}) \text{ and } (\sigma_{ij} - u_w\delta_{ij})\end{array}\right\} \tag{8}$$

iii. Effective stress of the Bishop type combined with other stress state variables taking either of the following forms:

$$\text{Form A: } \left\{\begin{array}{l}\sigma_{ij}^{'} = (\sigma_{ij} - u_a\delta_{ij}) + \overline{\mu}(s)\delta_{ij} \\ \xi_{ij} = \overline{\xi}(s, S_r)\delta_{ij}\end{array}\right\} \tag{9}$$

$$\text{Form B: } \left\{\begin{array}{l}\sigma_{ij}^{'} = (\sigma_{ij} - u_a\delta_{ij}) + \overline{\mu}_2(s, S_r)\delta_{ij} \\ \xi_{ij} = \overline{\xi}(s, S_r)\delta_{ij}\end{array}\right\} \tag{10}$$

Where μ_1 and μ_2 are defined as functions of suction *(s)* and degree of saturation *(S_r)*.

Successful implementation of unsaturated soil mechanics into engineering practices demands better understanding of parameters that control unsaturated behavior. Equally important is to understand how each parameter influences the volumetric or strength properties of the unsaturated media. For example, better realization of matric suction and fabric (skeletal or pore-fluid) enables better conceptualization of the bulk soil behavior. In this regard, understanding and quantifying the evolution of the pore-water fabric for unsaturated soil with changes in suction and saturation could help explain many of the anomalies that have plagued existing unsaturated effective stress formulations (Jennings & Burland 1962; Nuth & Laloui 2008).

Ongoing work has indicated that models incorporating only net normal stress and matric suction in their formulation are unlikely to fully capture all aspects (e.g. nonlinearity, hysteresis, etc.) of unsaturated soil behavior. As suction, saturation, wetting direction, and intergranular stress are all inherently coupled, formulations that include both suction and saturation in their formulation are most likely to capture unsaturated soil behavior in a robust way. In this respect it becomes imperative to understand and include the effects of suction and soil fabric in the effective stress formulation. Incorporating suction and fabric, Li (2003a) followed the virtual work principle and forwarded an effective stress formulation for unsaturated granular assemblies at a microstructural level. This approach is direct and opens the window for consideration of pore-fluid in the effective stress quantification. Because of the appropriateness of the fundamental principles applied, the virtual work approach is followed in this paper. Slight modifications are made while modeling the pore-water and attempts are made to support the mathematical formulation with experimental results and digital image processing of the microstructure from X-ray CT scanned images.

While we recognize that many problems in unsaturated soils involve fine grained soils and that inclusion of physicochemical forces are imperative for a fuller description of their mechanics, granular particles are specifically chosen to elicit the influence of fabric elements on the effective stress tensor. Within the above scope, this study seeks to advance the applicability of effective stress concepts for unsaturated soils with due regard to pore-fluid fabric and suction contributions at a microstructural level. The particular objective of this paper is to integrate microstructural features and measurements into a new effective stress formulation for unsaturated granular soils.

Matric suction

In geotechnical engineering suction can be defined as a quantity that quantify the thermodynamic potential of soil pore water relative to a reference potential of free water. Pore water potential may be imparted by capillary, osmotic and short-range adsorption effects. In granular assemblies, Figure 1, surface tension and interface curvature predominantly contribute to suction. Assuming the concentration of solute remains constant throughout (i.e. negligible osmotic contribution) the difference between water pressure (u_w) and air pressure (u_a), resulting from the surface tension and net negative pore pressure, is generally referred to as matric suction. In the absence of external load, the liquid bridge menisci (see Figure 1b) give rise to interparticle interactions. Molenkamp and Nazemi (2003a) named the resulting tensor "effective suction tensor". In a more recent study by Li (2003b, 2007a, 2007b), the suction tensor was shown to have a deviatoric part, that depends on the granular fabric, in addition to its isotropic part.

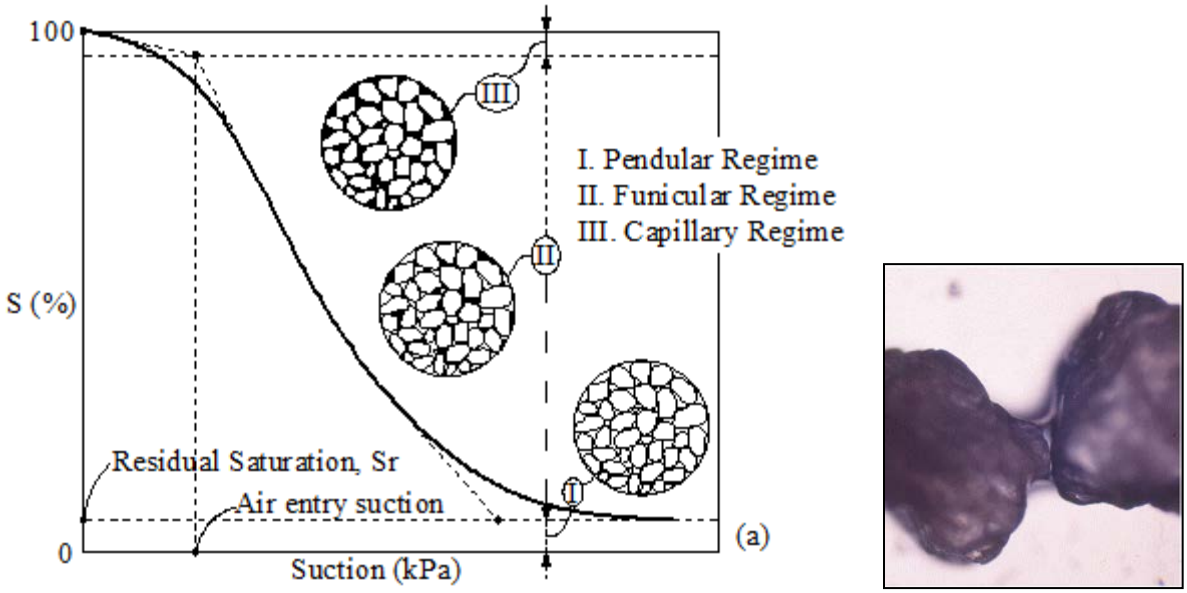

(a) (b)

Figure 1. (a) Regimes of soil water characteristic curve (SWCC) for partially saturated granular soil. (b) Meniscus between two granular particles (Fig. b modified from Gili 1988)

When granular materials are subjected to external loads, it is evident that granular fabric and the liquid bridge network will change. This evolution affects the state of stress and corresponding non-linear and hysteretic material behavior. Moreover, the wetting and suction histories have effects on shear strength and volume change behaviors (Ho 1988; Rahardjo 1990; Fredlund & Rahardjo 1993; Pereira 1996; Shuai F. 1996). Historically, suction was included in the effective stress formulation since the works of Aitchison and Donald (1956).

Soil fabric

Fabric is defined as a term referring to parameters like size, shape and arrangement of the solid particles, the organic inclusions and the associated voids (liquid or gas). Comprehensive description of fabric and its effect on the state of stress in different saturation regimes can be derived from micromechanics. Since early estimates of the liquid bridge force between monosized smooth spheres (Fisher 1926), several researches have advanced solutions for interactions between liquid bridges and rough rigid spheres or other geometries (Pietsch 1968; Lian et al. 1993; Likos & Lu 2004). In this regard: two-particle models have been extended to regular packings of isodiametral spheres to derive simple microstructural constitutive models for unsaturated granular media (Biarez et al. 1993; Molenkamp & Nazemi 2003a; Hicher & Cheng 2008); and particle-based computational simulations have been used to explore bulk behavior of unsaturated media for irregularly packed and polydisperse populations of spheres in 2-D and 3-D (Jiang et al. 2004; El-Shamy & Groger 2008). While such models have advanced our understanding of unsaturated soil microstructure and the applicability of effective stress concepts, they lack support from direct observation and quantification of microstructural features.

Mathematically, fabric had been defined (Scott 1963; Mitchell 1976; Muhunthan 1991) in a number of ways and a number of researchers (e.g. Cowin & Satake 1978; Nemat-Nasser & Mehrabadi 1983; Kanatani 1984, 1985) studied fabric tensor based on solid particles. An interesting remark by Muhunthan (1991) was that defining tensor parameters on the void phase of a partially saturated media has a potential of delivering a unified measure for all particulate media. Moreover, the advent of industrial X-ray CT and its applicability to the scanning of geomaterials has enabled distinct imaging of the solid, liquid and gas phases at a microstructural level. In this study, statistical correlations applicable to solid particles are assumed to appropriately describe directional quantities on the liquid phase.

Displacement field in granular assembly

In this section the displacement field, an important component in the formulation of the virtual work, is derived. To do so consider two particles A and B, with centroids at X^A and X^B respectively and touching at point C located at X^C, in contact in a granular assembly as shown in Figure 2. Let f_i^{AB} & f_i^{BA} be the forces exerted by particles A and B on each other. Equilibrium condition requires that

$$f_i^{AB} + f_i^{BA} = 0 \tag{11}$$

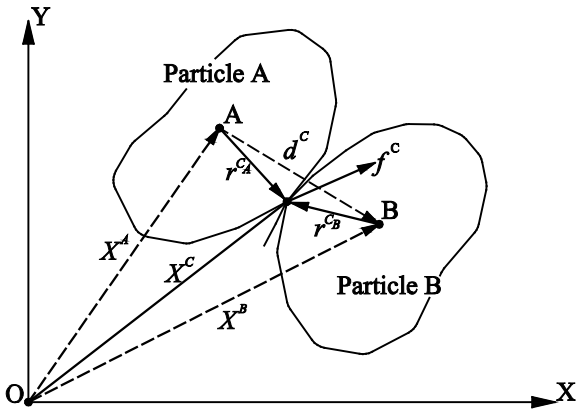

Figure 2. Solid particles in contact

If, in the assembly under a state of equilibrium, there are *n* numbers of particles in contact with particle A at point β representing the counter for the n contact points, we can write

$$\sum_{\beta=1}^{n} f_i^{A\beta} = 0 \tag{12}$$

Total moment in the assembly of particles in contact with A can be described as

$$\sum_{\beta=1}^{n} f_i^{A\beta}(x_j^{A\beta} - x_j^A) = \sum_{\beta=1}^{n} f_j^{A\beta}(x_i^{A\beta} - x_i^A) \tag{13}$$

Where, the moment contribution from each contact point is given by

$$\underbrace{f_i^{AB}(x_j^{AB} - x_j^A)}_{Particle\ A} + \underbrace{f_i^{BA}(x_j^{BA} - x_j^B)}_{Particle\ B} = f_i^C(x_j^B - x_j^A) \tag{14}$$

Considering all particles in the assembly touching at contact point *C* and denoting the total number of contact points in the assembly by *N*, the total moment may be written as

$$\sum_{C=1}^{N} f_i^C(x_j^B - x_j^A) = \sum_{C=1}^{N} f_i^C d_j^C \tag{15}$$

Where, $\left(x_j^B - x_j^A\right) = d_j^C = \left(r^{C_A} - r^{C_B}\right)$ is referred to as the branch vector and it connects the centroid of particles A and B.

Consider a virtual displacement field which introduces the relative displacement Δ_{ij}^C of the contact point *C*.

$$\text{i.e. } \Delta_{ij}^C = u_i^{CB} - u_i^{CA} \tag{16}$$

Where u_i^{CA} and u_i^{CB} are displacements of the contact point *C* when viewed as belonging to particle A and B respectively and written as

$$\left.\begin{aligned} u_i^{CA} &= u_i^A + \omega_{ij}^{AC}(x_j^C - x_j^A) \\ u_i^{CB} &= u_i^B + \omega_{ij}^{BC}(x_j^C - x_j^B) \end{aligned}\right\} \tag{17}$$

Where $\omega_{ij}^{AC} = -\omega_{ij}^{CA}$ and $\omega_{ij}^{BC} = -\omega_{ij}^{CB}$ represent the rotation of *C* relative to A and B respectively; u_i^A and u_i^B are the displacements of the centroid of A and B respectively. Inserting Equation 17 into the expression for Δ_{ij}^C leads to

$$\begin{aligned}\Delta_{ij}^C &= \left\{u_i^B + \omega_{ij}^{BC}(x_j^C - x_j^B)\right\} - \left\{u_i^A + \omega_{ij}^{AC}(x_j^C - x_j^A)\right\} \\ &= \left\{u_i^B - u_i^A\right\} + \omega_{ij}^{BC}(x_j^C - x_j^B) - \omega_{ij}^{AC}(x_j^C - x_j^A)\end{aligned} \tag{18}$$

In Equation 18, denoting u_i at the contact point *C* by $u_i^C = u_i(x^C)$; the rotation of contact point C as viewed from A and B by $\omega_{ij}^{AC} = \omega_{ij}^{BC} = \omega_{ij}(x^C)$ and assuming the displacement u_i and the associated rotations ω_{ij}^{AC} and ω_{ij}^{BC} conform to some smooth fields u_i and ω_{ij} hence a uniform strain field exists (i.e. continuous deformation is assumed so that a differentiable function can be obtained) one can get

$$\Delta_{ij}^C = \left(u_i^B - u_i^C\right) - \left(u_i^A - u_i^C\right) + \omega_{ij}^{CA}(x_j^C - x_j^A) - \omega_{ij}^{CB}(x_j^C - x_j^B) \tag{19}$$

Where $\left(u_i^B - u_i^C\right) = \frac{\partial u_i}{\partial x_j}(x^C)(x_j^B - x_j^C)$ and $\left(u_i^A - u_i^C\right) = \frac{\partial u_i}{\partial x_j}(x^C)(x_j^A - x_j^C)$ represent the contact to centroid distances of particles A & B respectively. Inserting these set of equation into the expression given by Equation 19 leads to

$$\Delta_{ij}^C = \frac{\partial u_i}{\partial x_j}(x^C)(x_j^B - x_j^C) - \frac{\partial u_i}{\partial x_j}(x^C)(x_j^A - x_j^C) + \omega_{ij}(x^C)(x_j^C - x_j^B) - \omega_{ij}(x^C)(x_j^C - x_j^A)$$

$$\Delta_{ij}^C = \frac{\partial u_i}{\partial x_j}(x^C)\left\{x_j^B - x_j^C - x_j^A + x_j^C\right\} + \omega_{ij}(x^C)\left\{x_j^C - x_j^A - x_j^C + x_j^B\right\}$$

$$\Delta_{ij}^C = \left\{\frac{\partial u_i}{\partial x_j}(x^C) - \omega_{ij}(x^C)\right\}\left(x_j^B - x_j^A\right)$$

$$\Delta_{ij}^C = \left\{\frac{\partial u_i}{\partial x_j}(x^C) - \omega_{ij}(x^C)\right\}\left(d_j^C\right) \tag{20}$$

Furthermore a linear boundary displacement can assumed in the uniform strain field such that

$$u_i = \phi_{ij} x_j + c_i \tag{21}$$

Where ϕ_{ij} is an arbitrary second order constant tensor and c_i is a constant vector. With this assumption applied to Equation 20 it can be shown, to a first order of approximation, that the displacement field is given by

$$\Delta_{ij}^C = \left\{ \frac{\partial u_i}{\partial x_j}(x^C) - \omega_{ij}(x^C) \right\} \left(d_j^C \right) = -\left(u_{i,j} + e_{ijk}\omega_k \right) d_j^C = \phi_{ij} d_j^C \tag{22}$$

The principle of virtual work

Virtual work principle is applied to relate contact forces to the overall stress in partially saturated granular assemblies. To accomplish this, basic assumptions of: regarding soil skeleton as an assembly of arbitrary rigid body particles in contact to each other; neglecting the effect of microcouples produced at particle contacts; ignoring body forces; continuous displacement of particles in an assembly during macroscopic deformation have been made. Referring to the partially saturated granular assembly and its associated microstructural force system shown in Figure 3, it can be said that virtual work can be done by three groups of forces in the representative elementary volume (REV). The total virtual work done can be assumed to be the sum of the work done by the paired internal contact forces f_i and $-f_i$; the boundary contact forces $\hat{f}_i$ that result from direct contact with particles from other REV*;* and surface traction p_i that result from pore pressure u_a or u_w. Each component will be discussed in subsequent sections of this paper.

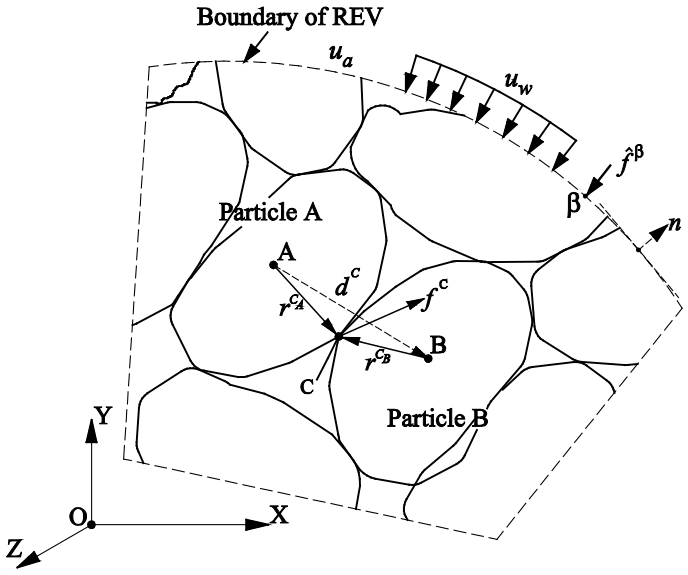

Figure 3. The force system of a three-phase granular assembly

Virtual work done by internal contact forces: We have defined f_i^C and $-f_i^C$ as the contact forces exerted on particle A and B by each other at contact point *C*. And $\Delta_i^C = \phi_{ij} d_j^C$ as indicated in Equation 22 represents the virtual relative displacement at *C*. The virtual work done, by the paired and opposite contact forces f_i^C and $-f_i^C$, is thus given as:

$$f_i^C \Delta_i^C = \phi_{ij} (f_i^C d_j^C) \tag{23}$$

The total work done by all internal contact forces at particle "A" will then be the sum of all contributions from each contact and this may be expressed as:

$$\sum_1^N f_i^C \Delta_i^C = \phi_{ij} \sum_1^N f_i^C \Delta_j^C = -\left(u_{i,j} + e_{ijk} \omega_k \right) \sum_1^N f_i^C \Delta_j^C \tag{24}$$

Where *N* represents the total number of internal contact points of particle A with its neighbors.

Substituting the expression defined for Δ_j^C into Equation 24 one may write the expression of the work done by all internal contact forces in the granular assembly as

$$\phi_{ij} \sum_1^N f_i^C (r_j^{C_A} - r_j^{C_B}) = \phi_{ij} \sum_1^N \left\{ f_i^C r_j^{C_A} + (-f_i^C r_j^{C_B}) \right\} = \phi_{ij} \sum_1^P \sum_1^N f_i^{P_C} r_j^{P_C} = -\left(u_{i,j} + e_{ijk} \omega_k \right) \sum_1^P \sum_1^N f_i^{P_C} r_j^{P_C} \tag{25}$$

Where P is the total number of particles in the REV; $f_i^{P_C}$ is the force acting on particle P at C; and $r_j^{P_C}$ is the vector that connects the centroid of P to C.

Virtual work done by boundary contact forces: The second group of forces that contribute to the total virtual work consists of the contact forces on an imaginary bounding surface that separates neighboring REVs (see Figure 3). The virtual work done by these groups of forces $\hat{f}_i$ can be written as follows (Li 2003a):

$$W^b = \sum_{\beta=1}^{k} \hat{f}_i^{\beta} u_i^{\beta} = u_{i,j} \sum_{\beta=1}^{k} \hat{f}_i^{\beta} x_j^{\beta} \tag{26}$$

Where k is the total number of concentrated contact forces acting on the boundary of the REV; $\hat{f}_i^{\beta}$ is the magnitude of the contact force; and x_j^{β} is the position vector at contact point β.

Virtual work done by pore pressure on particle surfaces: This group of forces is composed of pore-pressures acting on particle surfaces. The pore-pressure is distributed force acting on an area and thus its computation demands integration over the particle-pore contact area. Following the formulation by Li (2003a), the virtual work done by the particle surface traction, p_i from this group can be written as

$$\sum_{1}^{P} \int_{S^P} p_i u_i dA = \sum_{1}^{P} \int_{S^P} p_i (u_{i,j} x_j^{c_P} - e_{ijk} \omega_k r_j^P) dA = u_{i,j} \sum_{1}^{P} x_j^{c_P} \int_{S^P} p_i dA - e_{ijk} \omega_k \sum_{1}^{P} \int_{S^P} p_i r_j^P dA \tag{27}$$

Where S^P is the surface area of particle P in contact with pore-fluid (water or air) and r_j^P is the radial vector from the particle centroid $x_j^{c_P}$ to a point on S^P. If we assume the surface traction to be composed of contributions from air and water, we can let

$$p_i = \left[S_r u_w + (1 - S_r) u_a \right] \delta_{ij} n_j = \left[S_r u_w + (1 - S_r) u_a \right] n_i \tag{28}$$

When inserted into Equation 27, this leads to

$$\sum_{1}^{P}\int_{S^P} p_i u_i dA = u_{i,j}\sum_{1}^{P} x_j^{c_P}\int_{S^P}\left\{u_a-\left(u_a-u_w\right)S_r\right\}n_i dA - e_{ijk}\omega_k\sum_{1}^{P}\int_{S^P}\left\{u_a-\left(u_a-u_w\right)S_r\right\}n_i r_j^P dA \tag{29}$$

Total virtual work: Summing the contributions from internal contact forces, boundary contact forces, and the pore-pressure yields the total virtual work done, *W*, in the REV and this can be written as

$$\begin{aligned} W &= \phi_{ij}\sum_{1}^{P}\sum_{1}^{N} f_i^{P_C} r_j^{P_C} + u_{i,j}\sum_{\beta=1}^{k}\hat{f}_i^{\beta} x_j^{\beta} + \sum_{1}^{P}\int_{S^P} p_i u_i dA \\ &= \left\{-\left(u_{i,j}+e_{ijk}\omega_k\right)\sum_{1}^{P}\sum_{1}^{N} f_i^{P_C} r_j^{P_C}\right\} + \left\{u_{i,j}\sum_{\beta=1}^{k}\hat{f}_i^{\beta} x_j^{\beta}\right\} \\ &+ \left\{u_{i,j}\sum_{1}^{P} x_j^{c_P}\int_{S^P}\left\{u_a-\left(u_a-u_w\right)S_r\right\}n_i dA - e_{ijk}\omega_k\sum_{1}^{P}\int_{S^P}\left\{u_a-\left(u_a-u_w\right)S_r\right\}n_i r_j^P dA\right\} \end{aligned} \tag{30}$$

At particle and system equilibrium, the magnitudes of the resultant moment on each particle and total virtual work done in the microstructural system are both zero. The superposition of these two conditions transforms the formulation to the virtual work equation for the soil skeleton. Particle equilibrium (i.e. no translation and rotation) condition leads to zero resultant moment given as

$$e_{ijk}\left(\sum_{1}^{N} f_i^{P_C} r_j^{P_C} + \int_{S^P} p_i r_j^P dA\right) \equiv 0 \tag{31}$$

Applying this to the total virtual work equation and considering system equilibrium conditions (i.e. W = 0), we get what is referred to as the virtual work equation for the soil skeleton as follows

$$\begin{aligned} 0 &\equiv -u_{i,j}\sum_{1}^{P}\sum_{1}^{N} f_i^{P_C} r_j^{P_C} + u_{i,j}\sum_{\beta=1}^{k}\hat{f}_i^{\beta} x_j^{\beta} + u_{i,j}\sum_{1}^{P} x_j^{c_P}\int_{S^P} p_i dA \\ &\Leftrightarrow \sum_{1}^{P}\sum_{1}^{N} f_i^{P_C} r_j^{P_C} = \sum_{\beta=1}^{k}\hat{f}_i^{\beta} x_j^{\beta} + \sum_{1}^{P} x_j^{c_P}\int_{S^P}\left\{u_a-\left(u_a-u_w\right)S_r\right\}n_i dA \end{aligned} \tag{32}$$

Multiplying both sides by $\frac{-1}{V}$ and solving for $\frac{-1}{V}\sum_{\beta=1}^{k}\hat{f}_i^{\beta}x_j^{\beta}$ yields:

$$-\frac{1}{V}\sum_{\beta=1}^{k}\hat{f}_i^{\beta}x_j^{\beta}=-\frac{1}{V}\sum_{1}^{P}\sum_{1}^{N}f_i^{P_C}r_j^{P_C}+\frac{1}{V}\sum_{1}^{P}x_j^{c_P}\int_{S^P}\{S_r u_w+(1-S_r)u_a\}n_i dA \tag{33}$$

Application of Cauchy's formula and Gauss's divergence theorem: Consider a continuum subjected to overall surface traction T_i on its surface S and total stress τ_{ij} over its volume V as shown in Figure **4**.

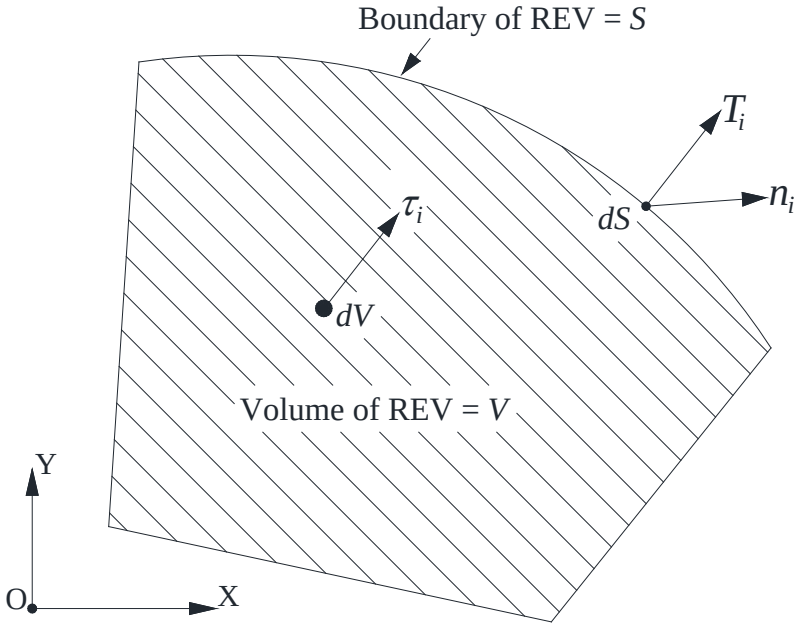

Figure 4. Representation of the REV as a continuum

It is possible to relate the overall stress to the contact forces by employing Cauchy's stress formula and Gauss's divergence theorem as

$$\begin{aligned}&\int_S T_i x_j dS=\int_S \tau_{ki}x_j n_k dS=\int_V \tau_{ki}x_{j,k}dV+\int_V \tau_{ki,k}x_j dV\\&\Rightarrow\int_S T_i x_j dS=\int_V \tau_{ki}x_{j,k}dV\\&\Rightarrow\int_S T_i x_j dS=\int_V \tau_{ji}dV\end{aligned} \tag{34}$$

Where τ_{ij} is the total stress in the continuum and n_k is the unit outward normal on S at x_j.

Recalling the assumption of the REV as statistically homogeneous, the total stress in the REV (σ_{ij}) can be computed as an average quantity as

$$\sigma_{ij} \triangleq \frac{-1}{V}\int_V \tau_{ij} dV \tag{35}$$

Applying divergence theorem, we can rewrite σ_{ij} as

$$\sigma_{ij} = \frac{-1}{V}\int_S T_j x_i dS \tag{36}$$

Remember that, in both equations, the negative sign is added to comply with the soil mechanics "compression-positive" sign convention.

Assuming that the air-water interface moves with the soil skeleton (i.e. its relative velocity will be negligible or zero), its contribution to the virtual work can be ignored (Houlsby 1997). Referring to Figure 3, surface traction T_i can be thought to be composed of the boundary contact forces, the pore-water pressure, and the pore-air pressure. In this regard, one can rewrite σ_{ij} as

$$\sigma_{ij} = \frac{-1}{V}\int_S T_j x_i dS = \frac{1}{V}\underbrace{\left\{-\sum_{\beta=1}^{k} \hat{f}_j^{\beta} x_i^{\beta}\right.}_{\substack{\text{Boundary contact} \\ \text{forces}}} + \underbrace{\int_S u_w n_j x_i dS}_{\substack{\text{Pore-water} \\ \text{pressure over} \\ \text{surface S}}} + \underbrace{\left.\int_S u_a n_j x_i dS\right\}}_{\substack{\text{Pore-air} \\ \text{pressure over} \\ \text{surface S}}} \tag{37}$$

Following the divergence theorem and noting that δ_{ij} is the kronecker delta we may rewrite the last two expressions in the right hand side of Equation 37 as

$$\frac{1}{V}\int_S \left(u_w + u_a\right) n_j x_i dS = \frac{1}{V}\delta_{ij}\int_V \left(u_w + u_a\right) dV \tag{38}$$

Moreover, considering the REV and introducing the degree of saturation S_r, the total pore-water and the pore-air pressures may be quantified as

$$\frac{1}{V}\delta_{ij}\int_V u_w dV = S_r u_w \delta_{ij} \tag{39}$$

$$\frac{1}{V}\delta_{ij}\int_V u_a dV = \left(1 - S_r\right) u_a \delta_{ij} \tag{40}$$

Substituting Equations 39 and 40 into 38 yields

$$\frac{1}{V}\delta_{ij}\int_V \left(u_w + u_a\right) dV = \left\{S_r u_w + \left(1 - S_r\right) u_a\right\} \delta_{ij} \tag{41}$$

Again inserting Equation 41 into the expression for the total stress (i.e. Equation 37) one gets

$$\sigma_{ij} = \frac{-1}{V}\int_S T_j x_i dS = -\frac{1}{V}\sum_{\beta=1}^{k} \hat{f}_j{}^{\beta} x_i{}^{\beta} + \left\{S_r u_w + \left(1 - S_r\right) u_a\right\} \delta_{ij} \tag{42}$$

Solving for the contribution by boundary forces (i.e. $\frac{-1}{V}\sum_{\beta=1}^{k} \hat{f}_i{}^{\beta} x_j{}^{\beta}$)

$$\frac{-1}{V}\sum_{\beta=1}^{k} \hat{f}_j{}^{\beta} x_i{}^{\beta} = \sigma_{ij} - \left\{S_r u_w + \left(1 - S_r\right) u_a\right\} \delta_{ij} \tag{43}$$

Recalling the expression we derived, using the virtual work principles (Equation 33), for the same quantity represented by Equation 43, and equating the two

$$-\frac{1}{V}\sum_{\beta=1}^{k} \hat{f}_i{}^{\beta} x_j^{\beta} = -\frac{1}{V}\sum_{1}^{P}\sum_{1}^{N} f_i^{P_C} r_j^{P_C} + \frac{1}{V}\sum_{1}^{P} x_j^{c_P} \int_{S^P} \left\{S_r u_w + (1 - S_r) u_a\right\} n_i dA = \sigma_{ij} - \left\{S_r u_w + \left(1 - S_r\right) u_a\right\} \delta_{ij}$$

$$\Rightarrow -\frac{1}{V}\sum_{1}^{P}\sum_{1}^{N} f_i^{P_C} r_j^{P_C} = \sigma_{ij} - \left[S_r u_w + \left(1 - S_r\right) u_a\right] \left\{\delta_{ij} + \frac{1}{V}\sum_{1}^{P} x_j^{c_P} \int_{S^P} n_i dA\right\} \tag{44}$$

Furthermore, if we introduce a second order tensor $F_{ij} = \left[\delta_{ij} + \frac{1}{V}\sum_{1}^{P} x_j^{c_P} \int_{S^P} n_i dA\right]$ that characterizes the distribution of pore-fabric, the above expression reduces to

$$-\frac{1}{V}\sum_{1}^{P}\sum_{1}^{N} f_i^{P_C} r_j^{P_C} = \sigma_{ij} - \left[S_r u_w + \left(1 - S_r\right) u_a\right] F_{ij} \tag{45}$$

Microstructure based effective stress for partially saturated granular soils

The following discussion will be based on Terzaghi's and Bishop's effective stress formulations for saturated and unsaturated soils respectively and proposes a definition to the effective stress pertinent to the microstructural context of this study.

Revisiting the effective stress formulations for saturated and unsaturated soils by Terzaghi (Equation 1) and Bishop (Equation 3) respectively, one can see that both formulations followed an argument in classical soil mechanics that the deformation and failure characteristics of a soil

are governed by the forces and constitutive properties at the particle contacts. Accordingly they inherently defined the "effective stress, $\sigma_{ij}^{'}$", as the fraction of the total stress carried by the soil solids (skeleton).

If we write the total stress in partially saturated soils as a sum of the stress carried by the distinct phases (i.e. solids, liquid and air) we get:

$$\sigma_{total} = \sigma_{solids} + \sigma_{liquid} + \sigma_{air} \tag{46}$$

Solving for the portion of stress carried by the soil skeleton:

$$\sigma_{solids} = \sigma_{total} - (\sigma_{liquid} + \sigma_{air}) \tag{47}$$

Comparison of this expression with the skeletal stress equation (Equation 45) obtained by combining the principles of virtual work and continuum theory on an REV, yields:

- $\frac{1}{V}\sum_{1}^{P}\sum_{1}^{N} f_i^{P_C} r_j^{P_C}$ as the stress carried by the solids
- $S_r u_w F_{ij}$ as the stress carried by the liquid and
- $(1-S_r)u_a F_{ij}$ as the stress carried by the air

Following Terzaghi's and Bishop's approach and expressing the effective stress as the skeletal or solid-phase stress we may write, with no loss of legitimacy,

$$\sigma_{ij}^{'} = \sigma_{ij} - S_r u_w F_{ij} - (1-S_r)u_a F_{ij} \tag{48}$$

Rearranging yields the effective stress formulation as proposed by this paper.

$$\sigma_{ij}^{'} = (\sigma_{ij} - u_a F_{ij}) + (u_a - u_w) S_r F_{ij} \tag{49}$$

Experimental determination of the fabric tensor

This section discusses a combined experimental and analytical approach to quantify component parameters in the proposed effective stress formulation. First, a brief description of the experimental setup is given. Then the procedures followed to quantify fabric tensor at different locations of the specimen will be discussed. Finally data obtained from the experimental and

analytical operations are presented and interpreted in terms of the proposed effective stress formulation.

An integrated system that consists of an X-ray CT scanner, a sample cell, 3-D imaging software, and automated imaging algorithms is utilized for data collection and nondestructive characterization. Laboratory tests include saturation and drying of specimens inside a specially designed suction-controlled cell with concurrent X-ray CT scanning. The integrated sample cell and X-ray CT system used in this study are shown in Figure 5.

In the scanning process the relative position of the sample between the detector and the X-ray source governs the spatial imaging resolution. In the experiments reported here, object and detector distances were set to be 62 mm and 1048 mm respectively to produce a corresponding spatial resolution of 30 μm. Information on the scan energy and flux is given in Table 1.

Glass beads, of sizes between 0.25 mm and 0.60 mm were graded as shown in the grain size distribution curve (ASTM C136-06) in Figure 6, with specific gravity of 2.50 were used to prepare a partially saturated specimen for the study. The specimen was compacted to an initial void ratio of 0.40. The height of the compacted specimen was measured to be 225 mm. The inside diameter of the sample cell was 12.46 mm and the total mass of the glass beads used was 49 grams. Pore-water was doped with CsCl (3% by weight) to increase the attenuation of X-rays on the liquid phase and ensure better contrast of the liquid phase (Willson et al. 2012).

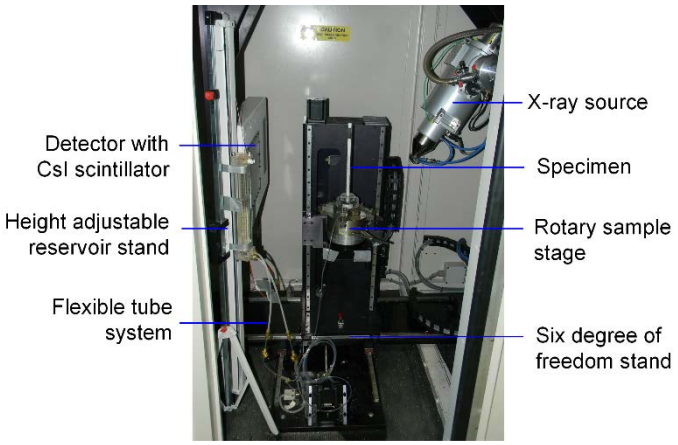

Figure 5. Experimental setup consisting of specially designed sample cell and X-ray CT scanning system

Table 1. X-ray CT scan data

Stage	Energy (keV)	Current (μA)
1	155	145
2	155	145
3	165	145
4	170	145

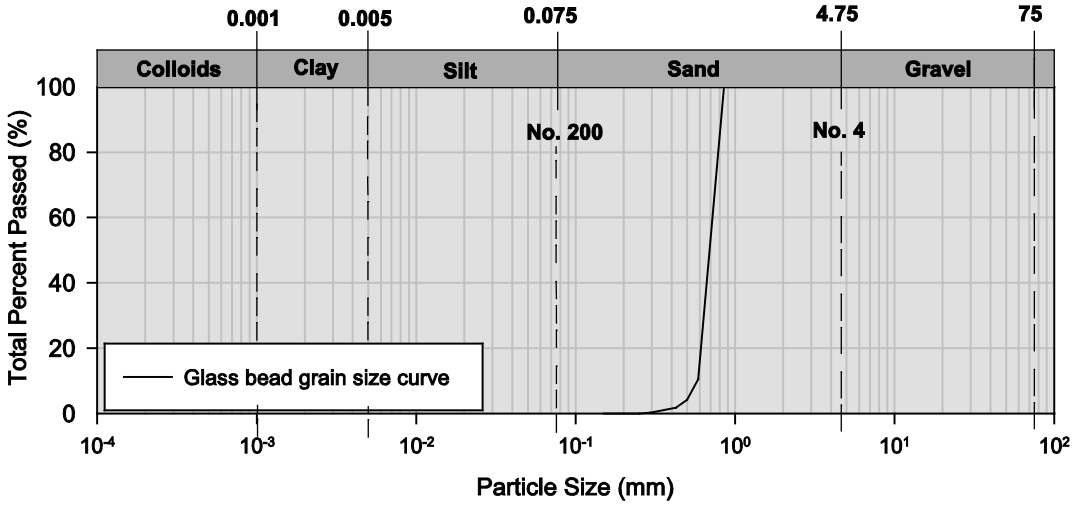

Figure 6. Grain size distribution for the glass bead material

The partially saturated specimen was scanned in four stages, two along a drying path and two along a wetting path, to obtain images of granular and fluid microstructure along the entire range

of the soil water retention curve (SWRC). Matric suction was applied to the specimen by integrating a high-air-entry cellulose membrane into the base of the sample column and applying suction using a hanging column system (ASTM D6836-02). In all stages reference datum was fixed and the location of water inside the specimen was carefully marked and used in calibrating the variation of suction inside the cell. The matric suction was quantified by correlating 100 kPa to 1020 cm of H_2O. A small opening was provided at the top of the sample cell to ensure the air pressure was atmospheric. In the presented work, where the suction range is small but sufficient for granular soil characterization, the deformation (swelling/collapse) of the soil during the drying and wetting processes was assumed insignificant.

The degree of saturation was obtained from digital image processing by means of local methods of thresholding and counting procedures. Macros in which the grey values of the air and liquid phase are specified were used to tell the image processing platform (Image-Pro Plus®) which voxel to count and accumulate. Finally, the degree of saturation values were expressed as percentages by taking the ratios of the voxel counts corresponding to the liquid phase, V_L, and void (air plus liquid) phase, V_V.

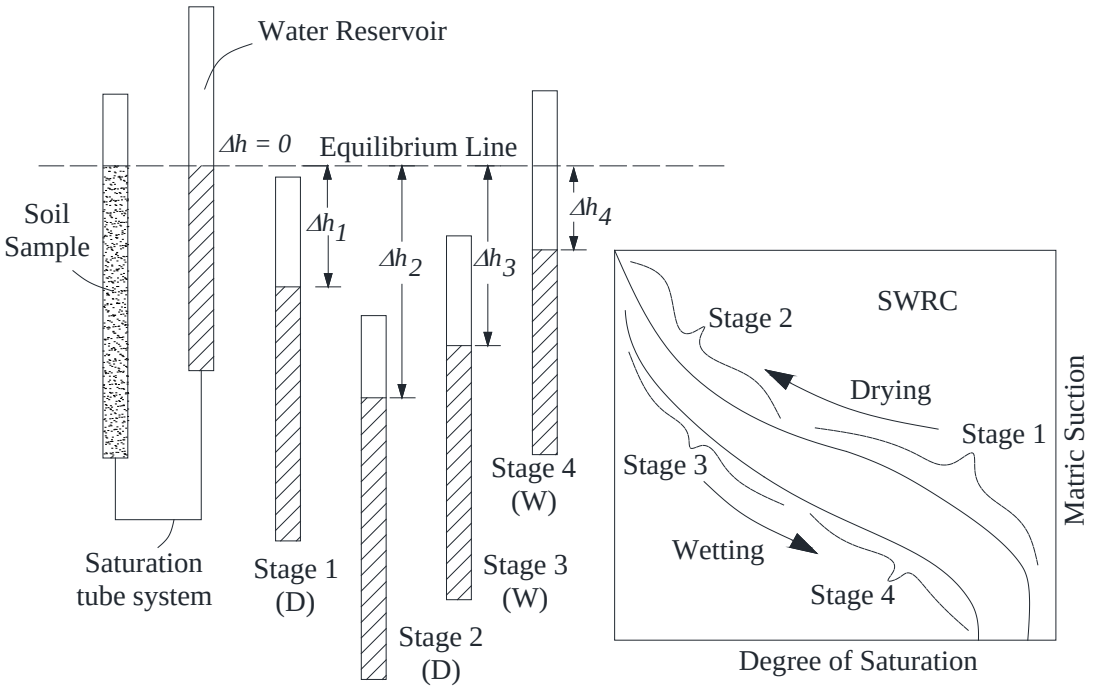

Figure 7. Schematics for the suction and wetting direction controlled experimental setup and the points represented by each stage

Figure 7 shows schematically how the four scanning stages were implemented. Stage 1 represents the initiation of drying of the specimen from its fully saturated condition. In this stage the suction head was set to 7 cm. In Stage 2 the water reservoir in the hanging column was lowered to a total head difference of 21.5 cm and hence cause further drying the sample. Stage 3 represents initiation of re-wetting of the sample. This was achieved by raising the water reservoir such that the head difference at equilibrium was reduced to 12 cm. Finally, in Stage 4 the suction head was further reduced to 4 cm to continue the wetting path. Data for measured suction and calculated saturation are presented in Table 2.The resulting SWRC, fitted with Van Genuchten's (1980) model, is shown in Figure 8. In the equation associated with the image, Θ_s and Θ_r are the saturations corresponding to the full and residual water contents respectively. ψ is the matric suction, α is a parameter related to the inverse of the air-entry suction, and *n* is a non-dimensional measure of the pore-size distribution.

Table 2. Measured suction and calculated degree of saturation

Stages	Suction (kPa)	Saturation (%)
Stage 1 (Drying)	0.000	97.34
	0.069	97.18
	0.201	97.04
	0.333	95.70
	0.466	85.50
Stage 2 (Drying)	0.588	66.75
	0.686	44.94
	0.784	35.17
	0.882	31.79
	1.176	21.24
	1.471	18.67
	1.765	6.74
	2.059	3.80
Stage 3 (Wetting)	1.127	1.28
	0.833	7.63
	0.588	12.42
	0.294	60.04
Stage 4 (Wetting)	0.343	38.40
	0.294	53.81
	0.196	82.21
	0.147	84.30
	0.098	86.40
	0.000	86.40

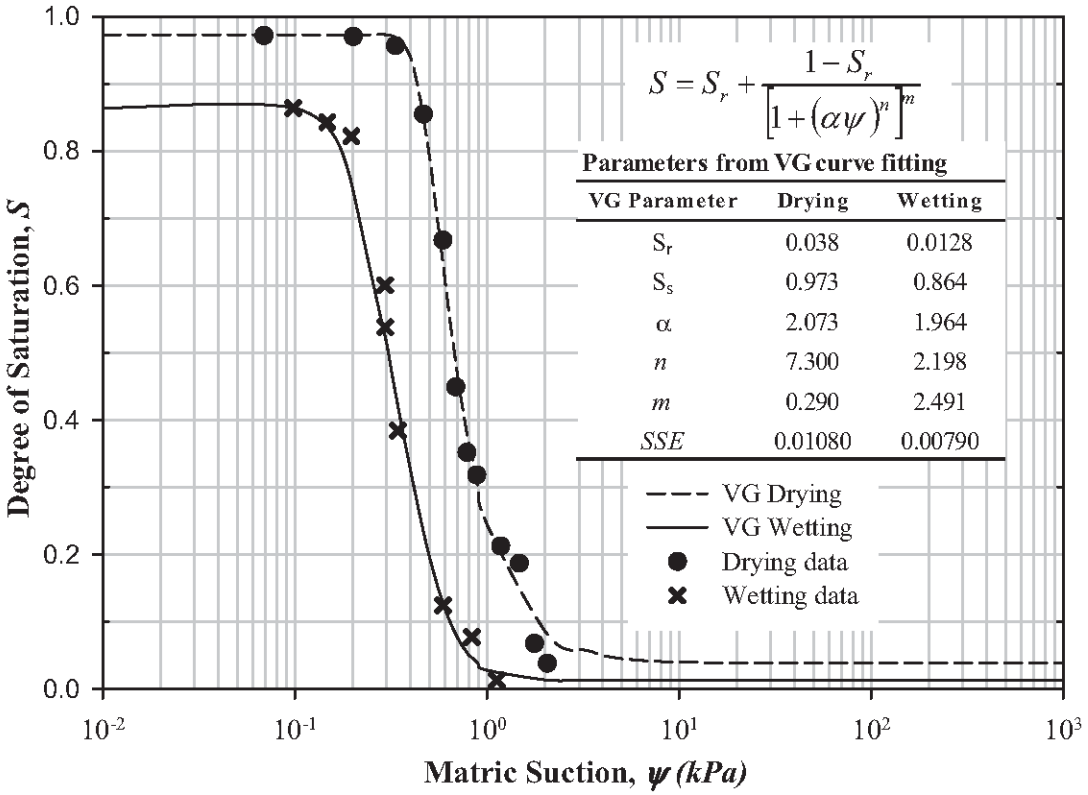

Figure 8. Soil water retention curve for the well graded glass bead

Following the procedures discussed in Manahiloh and Muhunthan (2012), the components of a second order fabric tensor N_{ij} were calculated for the liquid phase at the locations of the points given in Table 2. It should be noted that the fabric tensor F_{ij}, in the effective stress formulation, is a quantity different from Kanatani's fabric tensor of the second kind. F_{ij} can be related to N_{ij} by using tensorial operations (Boehler 1987) and this task is left for future work.

For demonstration consider the raw X-ray CT image shown in Figure 9a. By using thresholding and masking techniques, the liquid phase can be separated as shown in the segmented image in Figure 9b. The segmented liquid-phase image can then be discretized with watershed algorithms into a finite number of liquid cells as shown in Figure 9c. Each liquid cell can then be represented by a line element (i.e. by applying thinning techniques) aligned to the longest chord of a circumscribing ellipsoid as shown in Figure 9d and Figure 10. In Figure 10,

n_1 and n_2 represent the Cartesian components for a unit vector in the direction of the longest axis of the fitted ellipse and they can be written as

$$n_1 = \cos\theta^{(k)} \ \ldots \text{(a)} \qquad n_2 = \sin\theta^{(k)} \ldots \text{(b)} \tag{50}$$

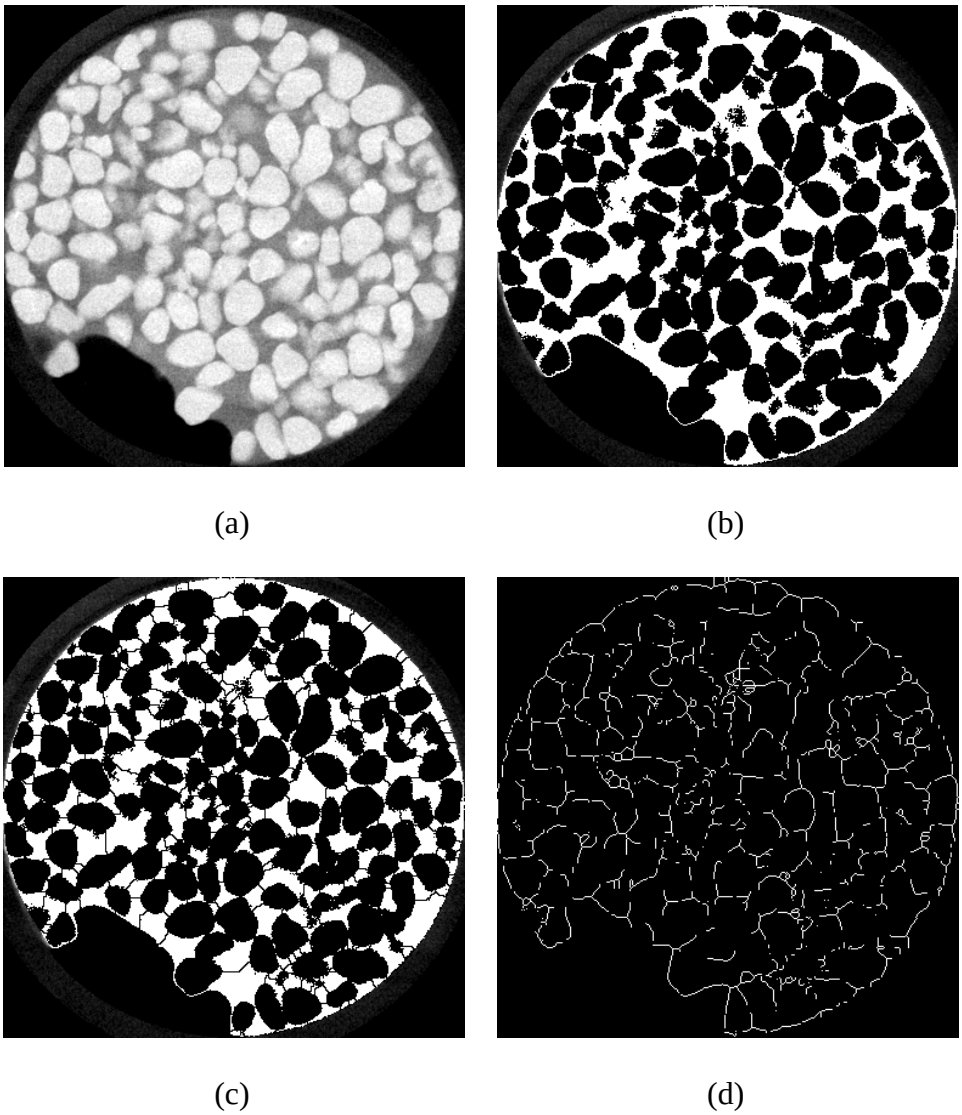

(a) (b)

(c) (d)

Figure 9. (a) Raw X-ray CT image; (b) Image segmented for liquid phase; (c) watershed applied to discretize the liquid phase; (d) Line represented liquid cells

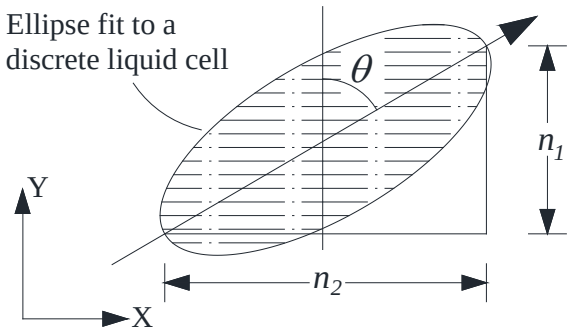

Figure 10. Alignment angle vector and components

The relative alignment, from the vertical, of the lines representing each discrete liquid cell can be quantified and used in the computation of the components of the second order fabric tensor as given in Equations 51 to 53. In the equations *M* represents the finite number of discretized liquid cells for which directional data is collected.

Adopting the approach of Oda and Nakayama (1989) and applying the automated image processing algorithms of Manahiloh and Muhunthan (2012), the components of the fabric tensor for the unsaturated glass bead system were calculated.

$$N_{11} = \frac{1}{M}\sum_{k=1}^{M}\cos^2\theta^{(k)} \tag{51}$$

$$N_{12} = \frac{1}{M}\sum_{k=1}^{M}\cos\theta^{(k)}\sin\theta^{(k)} \tag{52}$$

$$N_{22} = \frac{1}{M}\sum_{k=1}^{M}\sin^2\theta^{(k)} \tag{53}$$

Results are given in Table 3, where the last column reports values of the "vector magnitude" - an index that characterizes the intensity of preferred cell orientation (Curray 1956). Vector magnitudes (Δ) of 0 and 1 indicate no and maximum preference in orientation. Since its single value, obtained from Equation 54, is comprised of the contributions from the individual

components of the fabric tensor, it was chosen as a measure characterizing the variation of the fabric tensor.

$$\Delta = \frac{1}{M}\left[\sum_{k=1}^{M}\left(\cos 2\theta^{(k)}\right)^2 + \sum_{k=1}^{M}\left(\sin 2\theta^{(k)}\right)^2\right]^{1/2} \tag{54}$$

Plot of suction as a function of vector magnitude are shown in Figure 11and Figure 12 for the drying and wetting directions respectively. The figures present information on the trend followed in the variation of the vector magnitude as the suction/saturation changes. It can be seen that the vector magnitude stayed above 0.5 in both drying and wetting directions. Additionally, the orientation distribution of liquid cells varies randomly. This is an indication that suction greatly affects the preferred orientation of liquid cells inside a partially saturated specimen. Figure 13 and Figure 14 present the variations of the fabric tensor components, for both wetting and drying directions, as functions of suction and saturation respectively. The figures are presented to demonstrate the randomness of the variation of the component fabric tensors. However, on both figures one can observe that the magnitudes of N_{11} are greater in drying than wetting; the magnitudes of N_{22} are greater in wetting than drying and the magnitudes of N_{11} are greater than N_{22} in both wetting and drying.

Table 3. Fabric tensor components and vector magnitude

Stages	Suction (kPa)	Saturation S (%)	N_{11}	N_{12}	N_{22}	Δ
Stage 1 (Drying)	0.000	97.34	0.72182	0.00168	0.27818	0.666
	0.069	97.18	0.66940	0.00350	0.33060	0.582
	0.201	97.04	0.68784	-0.00234	0.31216	0.613
	0.333	95.70	0.78398	-0.00308	0.21602	0.754
	0.466	85.50	0.73296	-0.00150	0.26704	0.683
Stage 2 (Drying)	0.588	66.75	0.72642	-0.01248	0.27358	0.673
	0.686	44.94	0.81694	0.00746	0.18306	0.796
	0.784	35.17	0.76434	0.00200	0.23566	0.727
	0.882	31.79	0.83458	0.00432	0.16542	0.818
	1.176	21.24	0.88418	0.00202	0.11582	0.877
	1.471	18.67	0.83952	0.01764	0.16048	0.825
	1.765	6.74	0.96930	0.00008	0.03070	0.969
	2.059	3.80	0.98818	0.00012	0.01182	0.988
Stage 3 (Wetting)	1.127	1.28	1.00000	0.00000	0.00000	1.000
	0.833	7.63	0.97002	-0.00020	0.02998	0.970
	0.588	12.42	0.93424	-0.00006	0.06576	0.932
	0.294	60.04	0.73030	-0.00132	0.26970	0.679
Stage 4 (Wetting)	0.343	38.40	0.81464	0.00862	0.18536	0.793
	0.294	53.81	0.84844	0.00016	0.15156	0.835
	0.196	82.21	0.69000	0.00232	0.31000	0.616
	0.147	84.30	0.69384	-0.01088	0.30616	0.623
	0.098	86.40	0.68858	-0.01536	0.31142	0.615
	0.000	86.40	0.73368	-0.00252	0.26632	0.684

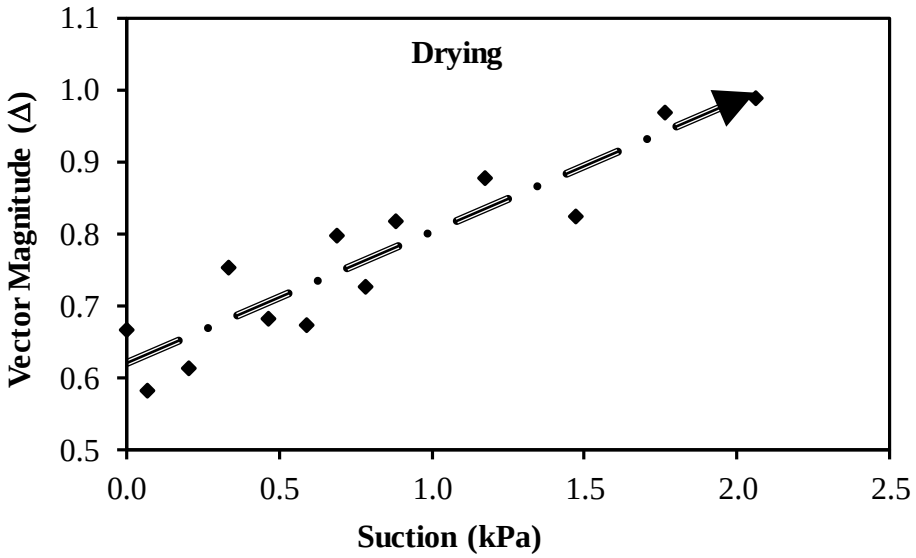

Figure 11. Variation of fabric tensor, as indexed by vector magnitude, along the drying path of the SWRC

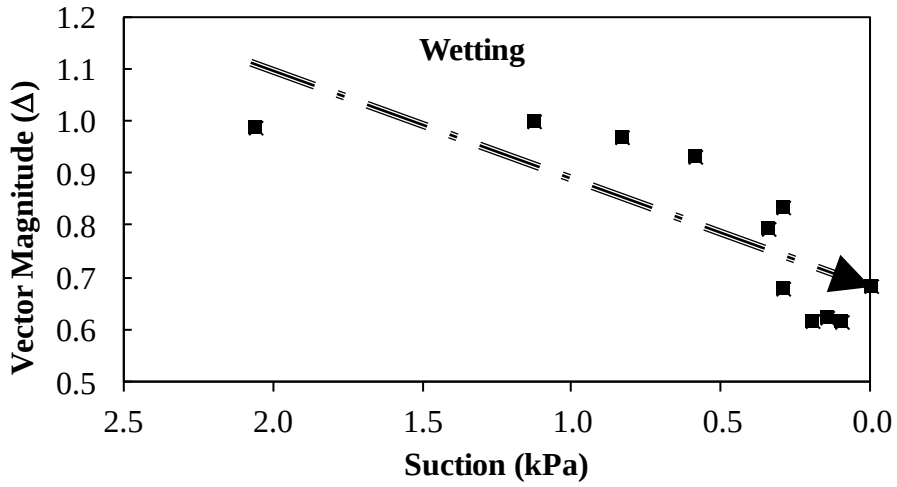

Figure 12. Variation of fabric tensor, as indexed by vector magnitude, along the wetting path of the SWRC

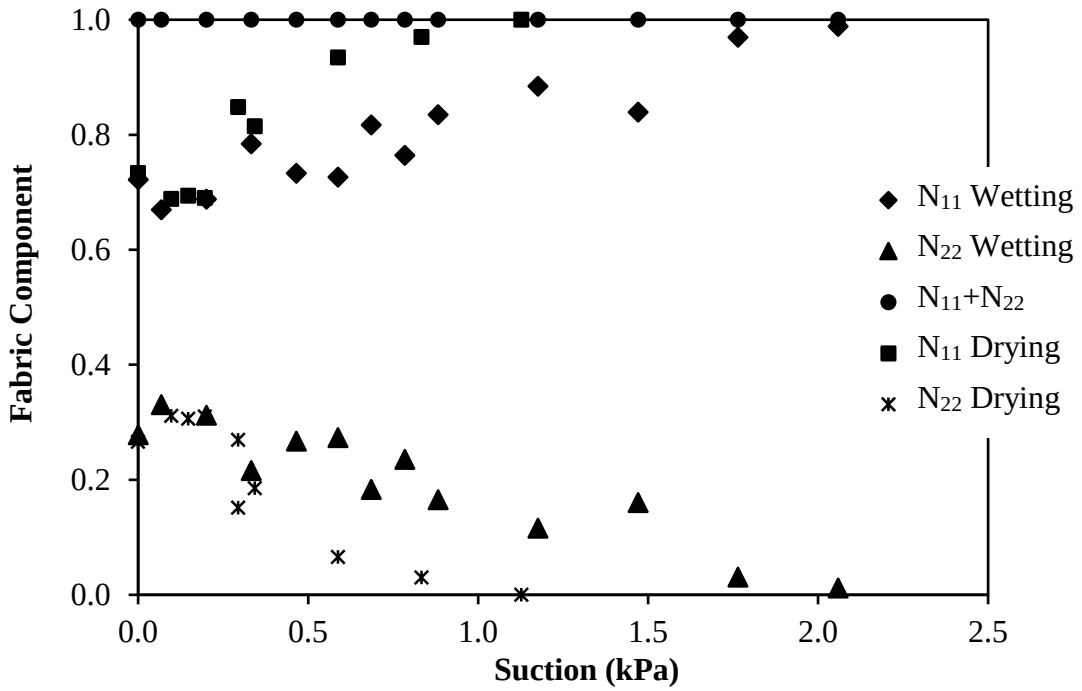

Figure 13. Variation of fabric tensor components as a function of suction

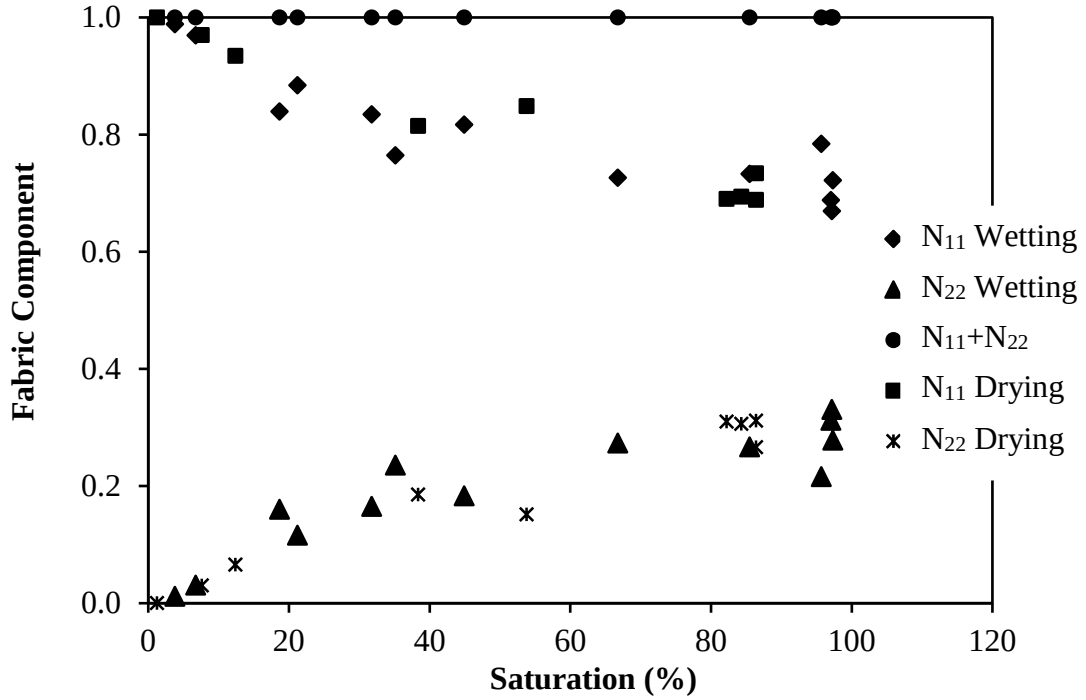

Figure 14. Variation of fabric tensor components as a function of saturation

It is evident from above observations that the orientation distribution of the liquid phase quantified by the fabric tensor continually varies. Such behavior influences the evolution of the effective stress to a greater extent and therefore effective stress formulations need to include this dynamic behavior. The effective stress formulation presented in this paper accounts for the fabric tensor and intrinsically relates its variation with suction and degree of saturation.

Summary and Conclusions

A new effective stress formulation that takes account of soil microstructure was proposed. In the derivation, following the work of Li (2003a), virtual work principles were adopted and Gauss's divergence theorem was implemented on Cauchy's stress formula to relate surface area and volume-related parameter definitions. The formulation meets the description of "Class iii" stress formulations as summarized by Nuth and Laloui (2008).

For fully saturated soils in which $S = 1$ and $F_{ij} = \delta_{ij}$, the proposed formulation reduces to the Terzaghi's and Bishop's (in which χ becomes 1) effective stress formulations as

$$\sigma_{ij}^{'} = \sigma_{ij} - u_a \delta_{ij} + \left(u_a - u_w\right)\delta_{ij} \tag{55}$$

It was shown that the effective stress is influenced by a second order fabric tensor that represents the spatial distribution of the liquid phase in the partially saturated system. This is in accordance with the Li (2003b) description of F_{ij} as the fabric tensor of the liquid phase.

In Li (2003a), a fabric tensor included in the effective stress formulation was expressed as an inherent function of the degree of saturation. Unlike Li (2003a), however, the formulation presented here has analytically de-coupled the two and expressed the fabric tensor independent of the degree of saturation. Variation of fabric tensor, and intrinsically the effective stress, was quantified as a function of suction and saturation.

The experimental description in the second half of this paper was presented neither as a direct means of quantifying F_{ij} nor a validation for the "correctness" of the proposed effective stress formulation. The intent was to show a procedure (that utilizes the advancements in the field of microstructural imaging and image processing) "potentially-expandable" towards the greater tasks of: (i) coming up with a working definition/interpretation of F_{ij}; (ii) developing a practical means of incorporating this definition into an effective stress formulation; and (iii) applying the formulation to models and designs that solve real-world-problems associated with unsaturated soils.

Acknowledgments

The work presented here is supported by the National Science Foundation (NSF) under the grant CMMI-0856793 to Washington State University and CMMI-1308110 to the University of Wisconsin-Madison. This support is gratefully acknowledged. Any opinions, findings, and conclusions or recommendations expressed in this material are those of the authors and do not necessarily reflect the views of NSF.

References

Aitchison, G.D., 1961, "Relationships of moisture stress and effective stress functions in unsaturated soils." *Pore pressure and suction in soils Conference,* British National Society of the International Society for Soil Mechanics and Foundation Engineering at the Institution of Civil Engineering, London, 47-52.

Aitchison, G.D., 1973, "The Quantitative Description of the Stress-Deformation of Expansive Soils - Preface to Set of Papers." *Proceedings of the 3rd International conference on expansive soils* Haifa, Israel, 79-82.

Aitchison, G.D., and Donald, I.B., 1956, "Effective stresses in unsaturated soils." *Proceedings of the 2nd Australia-New Zealand Conference on Soil Mechanics*, 192-199.

Alonso, E.E., Gens, A., and Hight, D.W., 1987, "Special problem soils: general report." *Proceedings of the 9th European Conference on Soil Mechanics and Foundation Engineering*Dublin, 1087-1146.

Alonso, E.E., Gens, A., and Josa, A., 1990, "A constitutive model for partially saturated soils," *Geotechnique*, Vol. 40(3), 405-430.

Alonso, E.E., Pereira, J.M., Vaunat, J., and Olivella, S., 2010, "A microstructurally based effective stress for unsaturated soils," *Geotechnique*, Vol. 60(12), 913-925.

ASTM C136-06, 2006, "Standard test method for sieve analysis of fine and coarse aggregates." ASTM International, West Conshohocken, PA.

ASTM D6836-02, 2008, "Standart test method for determination of the soil water characteristic curve for desorption using hanging column, pressure extractor, chilled mirror hygrometer, or centrifuge." ASTM International, West Conshohocken, PA.

Barden, L., Madedor, A.O., and Sides, G.R., 1969, "Volume Change Characteristics of Unsaturated Clay," *Journal of soil mechanics and foundation Div., ASCE*, Vol. 95(1), 33-51.

Berney, E.S., Engineers, U.S.A.C.o., Research, E., Center, D., Geotechnical, and Laboratory, S., 2004, *A Partially Saturated Constitutive Theory for Compacted Fills*, US Army Corps of Engineers, Engineer Research and Development Center, Geotechnical and Structures Laboratory.

Biarez, J., Fleureau, J.M., and Taibi, S., 1993, "Mechanical constitutive model for unsaturated granular media." *2nd International Conference on Micromechanics for Granular Media*Thorton, Balkema, London, 51-58.

Bishop, A.W., 1959, "The principle of effective stress," *Teknisk Ukeblad*, Vol. 106(39), 859-863.

Bishop, A.W., Alpan, I., Blight, G.E., and Donald, I.B., 1960, "Factors controlling the strength of partly saturated cohesive soils." *Proceedings of ASCE Research Conference on Shear Strength of Cohesive Soils*Boulder, Colorado, 503-532.

Bishop, A.W., and Donald, I.B., 1961, "The experimental study of partly saturated soil in the triaxial apparatus." *Proceedings of the 5th International Conference on Soil Mechanics and Foundation Engineering* Paris, 13-21.

Bishop, A.W., and Eldin, G., 1950, "Undrained triaxial tests on saturated sands and their significance in the general theory of shear strength," *Geotechnique*, Vol. 2, 13-32.

Boehler, J.P., 1987, *Applications of tensor functions in solid mechanics*, Springer-Verlag, Wien; New York.

Brackley, I.J.A., 1971, " Partial Collapse in Unsaturated Expansive Clay " *Proceddings of the 5th Regional Conference on Soil Mechanics and Foundation Engineering* South Africa, 23-30.

Burland, J.B., 1964, "Effective stresses in partly saturated soils, discussion of some aspects of effective stress in saturated and partly saturated soils by G.E. Blight and A.W. Bishop," *Geotechnique*, Vol. 14(2), 65-68.

Burland, J.B., 1965, "Some Aspects of the Mechanical Behaviour of Partly Saturated Soils." *Moisture Equilibria and Moisture Change in Soil beneath Covered Areas, A Sypposium in print. Edited by G.D. Aitchison*, Butterworths, Australia, 270-278.

Coleman, J.D., 1962, "Stress/Strain Relation for Partly Saturated Soils. Correspondence," *Geotechnique*, Vol. 12(4), 348-350.

Cowin, S.C., and Satake, T., 1978, "Continuum mechanical and statistical approaches in the mechanics of granular materials." *Proceedings of the US-Japan Seminar*, Gakujutsu Bunken, Snedai, Tokyo, 350.

Croney, D., Coleman, J.D., and Black, W.P.M., 1958, *Studies of the Movement and Distribution of Water in Soil in Relation to Highway Design and Performance*, Transport and Road Research Laboratory.

Curray, J.R., 1956, "The analysis of two dimensional orientation data," *Journal of Geology*, Vol. 64, 117-131.

El-Shamy, U., and Groger, T., 2008, "Micromechanical aspects of the shear strength of wet granular materials," *International Journal for Numerical and Analytical Methods in Geomechanics*, Vol. 32, 1763-1790.

Fisher, R.A., 1926, "On the capillary forces in an ideal soil," *Journal of Agricultural Science*, Vol. 16, 492-505.

Fredlund, D.J., and Morgenstern, N.R., 1977, "Stress State Variables for unsaturated soils," *ASCE Journal of Geotechnical Engineering*, Vol. 103, 447-466.

Fredlund, D.J., and Rahardjo, H., 1993, *Soil Mechanics for unsaturated soils*, Wiley, New York.

Gili, J.A., 1988, "Modelo microestructural para medios granulares no saturados." Ph.D. dissertation, UPC, Barcelona.

Hicher, P.Y., and Cheng, C.S., 2008, "Elastic model for partially saturated granular materials," *Journal of Engineering Mechanics*, Vol. 134(6), 505-513.

Ho, D.Y.F., 1988, "The relationships between the volumetric deformation moduli of unsaturated soils." Ph.D. dissertation, University of Saskatchewan, Saskaton, Canada.

Houlsby, G., 2004, "Editorial," *Geotechnique*, Vol. 54(10), 615.

Houlsby, G.T., 1997, "The work input to an unsaturated granular material," *Geotechnique*, Vol. 47(1), 193-196.

Jennings, J.E., 1961, "A Revised effective stress law for use in the prediction of the behaviour of unsaturated soils." *Pore Pressure and Suction in Soils*, Butterworths, London, 26-30.

Jennings, J.E., and Burland, J.B., 1962, "Limitations to the use of effective stress in partly saturated soils," *Geotechnique*, Vol. 12(2), 125-144.

Jiang, M., Leroueil, S., and Konard, J., 2004, "Insight to shear strength functions of unsaturated granulates by DEM analyses," *Computers and Geotechnics*, Vol. 31, 473-489.

Kanatani, K.I., 1984, "Distribution of directional data and fabric tensors," *International Journal of Engineering Science*, Vol. 22, 149-164.

Kanatani, K.I., 1985, "Procedures for stereological estimation of structural anisotropy," *International Journal of Engineering Science*, Vol. 23(5), 587-598.

Khalili, N., Geiser, F., and Blight, G.E., 2004, "Effective stress in unsaturated soils: Review with new evidence," *International Journal of Geomechanics*, Vol. 4, 115-126.

Khalili, N., and Khabbaz, M.H., 1998 "A unique relationship for c for the determination of the shear strength of unsaturated soils," *Geotechnique*, Vol. 48(5), 681-687.

Lambe, T.W., 1960, "A mechanistic picture of shear strength in clay." *Proceedings of the ASCE Research Conference on Shear Strength of Cohesive Soils*University of Colorado, Boulder, CO, 555–580.

Laughton, A.S., 1955, "The Compaction of Ocean Sediments." Ph.D. dissertation, University ofCambridge, England.

Li, X.S., 2003a, "Effective stress in unsaturated soil: A microstructural analysis," *Geotechnique*, Vol. 53(2), 273-277.

Li, X.S., 2003b, "Tensorial nature of suction in unsaturated granular soil." *Proceedings of the 16th ASCE Engineering Mechanics Conference*University of Washington, Seattle, WA.

Li, X.S., 2007a, "Thermodynamics-based constitutive frammework for unsaturated soils1: Theory," *Geotechnique*, Vol. 57(5), 411-422.

Li, X.S., 2007b, "Thermodynamics-based constitutive frammework for unsaturated soils2: A basic triaxial model," *Geotechnique*, Vol. 57(5), 423-435.

Lian, G., Thornton, C., and Adams, M.J., 1993, "A theoretical study of the liquid bridge forces between two rigid spherical bodies," *Journal of Colloid and Interface Science*, Vol. 161, 138-147.

Likos, W.J., and Lu, N., 2004, "Hysteresis of capillary stress in unsaturated granular soil," *Journal of Engineering Mechanics*, Vol. 130(6), 646-655.

Lu, N., and Likos, W.J., 2004, *Unsaturated Soil Mechanics*, Wiley, Hoboken, New Jersey.

Manahiloh, K.N., and Muhunthan, B., 2012, "Characterizing liquid phase fabric of unsaturated specimens from X-ray computed tomography images." *Unsaturated Soils: Research and Applications Edited by C. Mancuso, C. Jommi and F. D'Onza*
C. Mancuso, C. Jommi, and F. D'Onza, eds., Springer-verlag Berlin Heidelberg, 71-80.

Matyas, E.L., and Radhakrishna, H.S., 1968, "Volume change characteristics of partially saturated soils," *Geotechnique,* Vol. 18(4), 432-448 .

Mitchell, J.K., 1976, *Fundamentals of soils behavior*, Wiley, New York.

Molenkamp, F., and Nazemi, A.H., 2003a, "Micromechanical considerations of unsaturated pyramidal packing," *Geotechnique,* Vol. 53(2), 195-206.

Muhunthan, B., 1991, "Micromechanics of steady state, collapse and stress-strain modeling of soils." Ph.D. dissertation, Perdue University, West Lafayette.

Nemat-Nasser, S., and Mehrabadi, M.M., 1983, "Stress and fabric in granular masses." *Mechanics of Granular Materials: New Models and Constitutive Relations*, J. T. Jenkins, and M. Satake, eds., Elsevier, Amsterdam, 1-8.

Nuth, M., and Laloui, L., 2008, "Effective stress concept in unsaturated soils: Clarification and validation of a unified framework," *International Journal for Numerical and Analytical Methods in Geomechanics*, Vol. 32(2), 771-801.

Oda, M., and Nakayama, H., 1989, "Yield function for soil with anisotropic fabric," *ASCE Journal of Engineering Mechanics*, Vol. 115(1), 89-104.

Pereira, J.H.F., 1996, "Numerical analysis of the mechanical behavior of collapsing earth dams during first reservoir filling." Ph.D. dissertation, University of Saskatchewan, Saskatoon, Canada.

Pietsch, W.B., 1968, "Tensile strength of granular materials," *Nature*, Vol. 217, 736-737.

Rahardjo, H., 1990, "The study of undrained and drained behaviour of unsaturated soils." Ph.D. dissertation, University of Saskatchewan, Saskatoon, Canada.

Rendulic, L., 1936, "Relation between void ratio and effective principal stress for a remolded silty clay." *Proceedings of the 1st International Conference on Soil Mechanics and Foundation Engineering*, 48-51.

Richards, B.G., 1985, "Moisture flow and equilibria in unsaturated soils for shallow foundation." Barton A.C.T: Institution of Engineers, Australia, 71-101 pp.

Scott, R.F., 1963, *Principles of soil mechanics,* Addison-Wesley, Massachusetts.

Shuai F., 1996, "Simulation of Swelling Pressure Measurements on Expansive Soils." Ph.D. dissertation, University of Saskatchewan, Saskatoon, Canada.

Skempton, A.W., 1961, "Effective Stress in Soils, Concrete and Rocks." *Conference on Pore Pressure*London, 4-16.

Terzaghi, K., 1936, "The Shearing Resistance of Saturated Soils and the Angle between the Planes of Shear." *1st International Conference on Soil Mechanics*Cambridge, MA, 54-56.

Toll, D.G., 1990, "A framework for unsaturated soil behavior," *Geotechnique*, Vol. 40(1), 31-44.

Van Genuchten, M.T., 1980, "A closed-form equation for predicting the hydraulic conductivity of unsaturated soils," *Soil Science Society of America Journal*, Vol. 44(5), 892-898.

Vaunat, J., Cante, J.C., Ledesma, A., and Gens, A., 2000, "A stress point algorithm for an elastoplastic model in unsaturated soils," *International Journal of Plasticity*, Vol. 16(2), 121-141.

Wheeler, S.J., and Sivakumar, V., 1993, "Development and application of a critical state model for unsaturated soils." *Predictive soil mechanics. Proceedings of the Wroth memorial symposium, 27-29 July 1992*St Catherine's College, Oxford, 709–728.

Wheeler, S.J., and Sivakumar, V., 1995, "An elasto-plastic critical state framework for unsaturated soils," *Geotechnique*, Vol. 45(1), 35–53.

Willson, C.S., Lu, N., and Likos, W.J., 2012, "Quantification of grain, pore, and fluid microstructure of unsaturated sand from X-ray computed tomography images," *Geotechnical Testing Journal*, Vol. 35(6), 911-923.

Wood, M., 2005, "Geotechnical modelling," *Bromhead Quarterly Journal of Engineering Geology & Hydrology*, Vol. 38(1), 110-111.

Zhang, X., and Lytton, R.L., 2006, "Stress State Variables for saturated and unsaturated soils." *Fourth International Conference on Unsaturated Soils*, G. A. Miller, C. E. Zapata, S. L. Houston, and D. G. Fredlund, eds., Geo-Institute of ASCE, Arizona, 2380-2391.